An analytical solution for the magneto-electro-elastic bimorph beam forced vibrations problem

2009 Smart Mater. Struct. 18 085012

(http://iopscience.iop.org/0964-1726/18/8/085012)

IOP Publishing Smart Materials and Structures

Smart Mater. Struct. **18** (2009) 085012 (14pp) doi:10.1088/0964-1726/18/8/085012

An analytical solution for the magneto-electro-elastic bimorph beam forced vibrations problem

A Milazzo, C Orlando and A Alaimo

Dipartimento di Ingegneria Strutturale Aerospaziale e Geotecnica, University of Palermo, Viale delle Scienze Edificio 8, Palermo 90128, Italy

E-mail: alberto.milazzo@unipa.it, c.orlando@unipa.it and a.alaimo@unipa.it

Received 13 February 2009, in final form 27 April 2009
Published 4 June 2009
Online at stacks.iop.org/SMS/18/085012

Abstract

Based on the Timoshenko beam theory and on the assumption that the electric and magnetic fields can be treated as steady, since elastic waves propagate very slowly with respect to electromagnetic ones, a general analytical solution for the transient analysis of a magneto-electro-elastic bimorph beam is obtained. General magneto-electric boundary conditions can be applied on the top and bottom surfaces of the beam, allowing us to study the response of the bilayer structure to electromagnetic stimuli. The model reveals that the magneto-electric loads enter the solution as an equivalent external bending moment per unit length and as time-dependent mechanical boundary conditions through the definition of the bending moment. Moreover, the influences of the electro-mechanic, magneto-mechanic and electromagnetic coupling on the stiffness of the bimorph stem from the computation of the beam equivalent stiffness constants. Free and forced vibration analyses of both multiphase and laminated magneto-electro-elastic composite beams are carried out to check the effectiveness and reliability of the proposed analytic solution.

1. Introduction

Magneto-electro-elastic composites have recently been gaining attention for their unique capability of converting energy among the elastic, electric and magnetic forms. They generate electric and magnetic fields if stretched and undergo deformation when electric or magnetic external loads are applied. Moreover, they are able to convert an applied magnetic field into an electric one and vice versa [1, 2]. This last feature is referred to as a magneto-electric effect, which is a peculiar characteristic of the whole composite. In fact, magneto-electro-elastic materials are built up by combining together piezoelectric and piezomagnetic phases which provide the composite with both electro-mechanical and magneto-mechanical coupling. Moreover, the coexistence of the piezoelectric and piezomagnetic effects, coupled through the elastic field, gives rise to magneto-electric coupling [3]. For these reasons, magneto-electro-elastic materials are exploited for the construction of magnetic field probes, wireless powering systems of micro-electro-mechanical devices, control of structural vibration, electric packaging, hydrophones, medical ultrasonic imaging, sensors and actuators [4–7].

Particulate, fiber reinforced and laminated magneto-electro-elastic composites have been studied, to look for the highest magneto-electric effect [3, 8]. The effects on the magneto-electric coupling strength of the sintering temperature, volume fraction of piezoelectric and piezomagnetic phases, layers arrangement and thickness ratio, as well as of the magnetostriction direction and the bias magnetic field have been investigated both experimentally and theoretically [7, 9–16]. The aforementioned investigations revealed the better magneto-electric coupling of the laminated configuration that began to be widely studied and developed as an effective smart device [8]. Both analytical and numerical techniques have been developed to characterize the static and dynamic response of magneto-electro-elastic media. Wang and Shen [17] derived the general solution for three-dimensional transversely isotropic magneto-electro-elastic media by using five potential functions and determined Green's functions for a half-space and the fundamental solution for a generalized dislocation. Green's functions for the two-

dimensional problem have been obtained by Guan and He [18] by means of Almansi's theorem, while Green's functions for infinite, two-phase and semi-infinite magneto-electro-elastic composites have been derived and presented in [19]. The exact solution for the statically loaded three-dimensional multilayered rectangular simply supported plate of magneto-electro-elastic composites has been computed by Pan [20] by means of the propagator matrix method. The propagator matrix method has also been employed to solve cylindrical bending and free vibrations problems as reported in [21–23]. Solutions for magneto-electro-elastic functionally graded structures have also been obtained. Pan and Han [24] derived the exact solution for a multilayered functionally graded rectangular plate in a simply supported configuration undergoing general mechanical, electric and magnetic static loads by using a pseudo-Stroh formalism and the propagator matrix method. The problem of functionally graded plane beams has been addressed by Huang and co-workers [25] by writing the stress, electric displacement and magnetic induction functions as quadratic functions of the longitudinal direction and by computing their distribution along the thickness direction through an integral approach. An approximate solution for the laminated magneto-electro-elastic two-dimensional plates has been obtained by Ramirez and co-workers [26] by combining the discrete layer approach with the Ritz method in such a way that the developed model does not depend on boundary conditions. A state-space approach has been employed to derive analytical solutions for multilayered magneto-electro-elastic media [4, 27], to study the free vibration behavior of a simply supported non-homogeneous rectangular plate [28] and to obtain the solution for the magneto-electric thermoelasticity problem of a non-homogeneous transversely isotropic rectangular plate undergoing bending deformations [29]. In order to model general boundary condition configurations, the use of numerical methods is required. Bhangale and Ganesan [30] derived a hybrid formulation for analyzing the free vibrations problem of magneto-electro-elastic functionally graded cylindrical shells, by using series expansions in the circumferential and axial directions and finite elements in the radial one. A FE model has been used by Buchanan [14, 31] to study the multilayer and multiphase magneto-electro-elastic materials response. Lage and co-workers [32] derived a mixed finite element approach, on the basis of the mixed Reissner variational principle, to model magneto-electro-elastic plates. An in-plane plate finite element was developed and employed by Annigeri and co-workers [33] to study the free vibration behavior of multiphase and layered magneto-electro-elastic beams with different configurations. A boundary element model for the magneto-electro-elastic two-dimensional problem has been developed by Ding and Jiang [34], who found the related fundamental solutions starting from the general harmonic potential solution. Three-dimensional Green's functions for transversely isotropic magneto-electro-elasticity and 3D BEM analysis of an annular plate were presented by Ding and co-workers [35]. A boundary integral formulation expressed in terms of generalized variables, in such a way that the magneto-electro-elastic governing equations can be written in a form that resembles the governing equations of classical elasticity and its multidomain BEM implementation for two-dimensional laminate configurations, has been developed and presented by Milazzo and co-workers in [36], where the related fundamental solutions have been derived by means of a modified Lekhnitskii's approach and presented in a compact matrix form. BE analyses of bimorph magneto-electro-elastic device have also been carried out and presented in [37] by Daví *et al*.

To the authors' knowledge, the problem of forced vibration of magneto-electro-elastic media, despite its importance in engineering applications, has been presented only in the work of Hou and Leung [38], where an analytical solution for orthotropic and radially polarized hollow cylinders has been derived and used to study the structure responses to mechanical and magneto-electric loads.

In the present paper the problem of forced vibration of a magneto-electro-elastic bimorph beam is addressed. The model is based on Timoshenko's beam theory [39], extended to the present problem by considering the magneto-electro-mechanical constitutive relationships and by assuming that no density charge and no density current act on the beam. Moreover, the electric and magnetic fields are treated as quasi-static and no damping effects have been taken into account. The fundamental assumptions and the derivation of the governing equations are presented in sections 2 and 3, respectively. The free vibration problem is solved in section 4 while the forced vibration solution, based on the Mindlin and Goodman procedure [40] to take into account time-varying boundary conditions, is obtained in section 5. Some representative results are presented for different beam configurations in section 6. Natural frequencies for a single layer particulate magneto-electro-elastic composite beam and for a piezoelectric/piezomagnetic laminated structure are obtained and compared with finite element data for a plane beam. The transient responses of bimorph beams under mechanical and magnetic loads are also presented in terms of the mean-line transverse displacements and electric and magnetic potential distributions along the beam top surface. The forced vibration solution is verified by comparing the present analytical model with numerical results obtained through the boundary element approach developed by Milazzo *et al* [36] to study magneto-electro-elastic laminates.

2. Fundamental assumptions

Let us consider a magneto-electro-elastic composite bimorph beam of length L and thickness h, having electric and magnetic poling directions parallel to the y-axis, see figure 1. The bimorph laminae are considered perfectly bonded from the mechanical, electric and magnetic point of view.

The elastic variables used to model the problem are the displacement components u and v, along the x and y axes respectively, the cross sectional rotation θ, and the stress and strain components σ_{xx}, σ_{xy}, γ_{xx} and γ_{xy}. Both the transverse displacement and cross sectional rotation are supposed to be a function of the x variable only. Moreover, according to the Timoshenko beam model [39], the effect of shear deformation

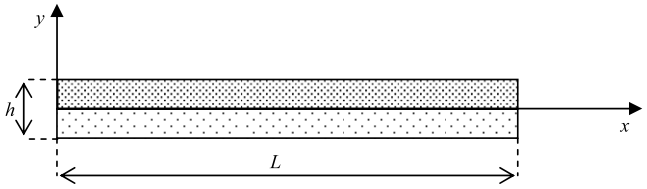

Figure 1. Bimorph geometry

is taken into account. It follows that, assuming the following kinematical model

$$u = -y\,\vartheta(x,t) \qquad v = v(x,t) \tag{1}$$

the considered strain components are given by

$$\gamma_{xx} = -y\frac{\partial \vartheta}{\partial x} \qquad \gamma_{xy} = -\vartheta + \frac{\partial v}{\partial x}. \tag{2}$$

The electric state of the body is described by the electric potential φ and by the electric field components E_x and E_y, that relate to electric potential as follows

$$E_x = -\frac{\partial \varphi}{\partial x} \qquad E_y = -\frac{\partial \varphi}{\partial y}. \tag{3}$$

On the other hand, in order to describe the magnetic state of the body, it is assumed that there is no external current density in the domain; thus, the magnetic field components, H_x and H_y, can be expressed in terms of a magnetic scalar potential ψ through the gradient relationships

$$H_x = -\frac{\partial \psi}{\partial x} \qquad H_y = -\frac{\partial \psi}{\partial y}. \tag{4}$$

The electric displacement vector components D_x and D_y and the magnetic induction vector components B_x and B_y, also used to describe the electric and magnetic state of the body, are obtained from the constitutive relationships. In accordance with the assumption made for piezoelectric devices in [41], the effect of the electric field component transverse to the poling direction, E_x, is considered negligible with respect to the electric field component along the poling direction E_y. This hypothesis is here extended to the magnetic problem by assuming that only the magnetic field component along the magnetic poling direction is relevant.

Under the aforementioned assumptions, the constitutive relationships for each lamina can be written as follows

$$\begin{aligned} \sigma_{xx} &= c\gamma_{xx} - eE_y - dH_y \qquad & \sigma_{xy} &= c_{44}\gamma_{xy} \\ D_x &= e_{14}\gamma_{xy} & D_y &= e\gamma_{xx} + \varepsilon E_y + \eta H_y \\ B_x &= d_{14}\gamma_{xy} & B_y &= d\gamma_{xx} + \eta E_y + \mu H_y \end{aligned} \tag{5}$$

where c and c_{44} are elastic stiffness constants, ε and μ are the dielectric constant and magnetic permeability, respectively, e and e_{14} represent the piezoelectric constants while the piezomagnetic coupling is expressed by the constitutive constants d and d_{14}; the last material constant η is representative of the magneto-electric coupling characteristic of the magneto-electro-elastic composite material. The complete constitutive relationships for a transversely isotropic magneto-electro-elastic material having electric and magnetic poling directions along the y-axis are listed in appendix A, where the expressions used to compute the constitutive constants for a monodimensional structure are also reported.

3. Model

The electromagnetic problem is firstly solved in terms of the displacement variables $v(x,t)$ and $\theta(x,t)$; then the magneto-electro-elastic problem is closed by using the equations of motion for the bimorph. It is assumed, by observing that the electromagnetic waves propagation velocity is several order of magnitude higher than that of elastic waves, that the electromagnetic state of the beam can be modeled as quasi-static. In what follows, variables denoted with a minus or plus superscript are intended to be related to the lower ($-h/2 \leqslant y \leqslant 0$) or upper ($0 \leqslant y \leqslant h/2$) lamina, respectively.

3.1. Magneto-electric problem

Gauss's laws for the electrostatic and magnetostatic, assuming that the electric charge is absent, state

$$\frac{\partial D_x}{\partial x} + \frac{\partial D_y}{\partial y} = 0 \qquad \frac{\partial B_x}{\partial x} + \frac{\partial B_y}{\partial y} = 0. \tag{6}$$

Taking into account the constitutive relationships, equations (5), the strain–displacement equations, equations (2) and the gradient relationships, equations (3) and (4), equations (6) lead to

$$\begin{aligned} \varphi^{\pm}(x,y,t) &= \left[A_{\varphi}^{\pm}\frac{\partial \vartheta}{\partial x} + B_{\varphi}^{\pm}\frac{\partial^2 v}{\partial x^2}\right]\frac{y^2}{2} + a_1^{\pm}y + a_2^{\pm} \\ \psi^{\pm}(x,y,t) &= \left[A_{\psi}^{\pm}\frac{\partial \vartheta}{\partial x} + B_{\psi}^{\pm}\frac{\partial^2 v}{\partial x^2}\right]\frac{y^2}{2} + a_3^{\pm}y + a_4^{\pm} \end{aligned} \tag{7}$$

where $a_i^{\pm}(i = 1,2,3,4)$ are integration constants while $A_j^{\pm}$ and $B_j^{\pm}(j = \varphi, \psi)$ are defined in appendix B equations (B.1). Since the interface has been considered electrically and magnetically perfect, the continuity conditions for both the electric and magnetic potentials and for the components of the electric displacement and of the magnetic induction normal to the interface are imposed, namely

$$\begin{aligned} &\varphi^{+}(y=0) = \varphi^{-}(y=0), \qquad \psi^{+}(y=0) = \psi^{-}(y=0) \\ &D_n^{+}(y=0) = D_n^{-}(y=0), \quad B_n^{+}(y=0) = B_n^{-}(y=0). \end{aligned} \tag{8}$$

It follows that the potentials integration constants belonging to lower lamina, a_i^- can be expressed in terms of the integration constants belonging to the upper lamina a_i^+ as

$$\begin{aligned} a_1^- &= Ca_1^+ + Da_3^+, \qquad & a_2^- &= a_2^+, \\ a_3^- &= Aa_1^+ + Ba_3^+, & a_4^- &= a_4^+ \end{aligned} \tag{9}$$

where A, B, C and D are combinations of the electromagnetic constitutive constants as reported in appendix B.

In order to determine the remaining integration constants a_i^+ the magneto-electric boundary conditions at the top and bottom surfaces of the bimorph beam are imposed. It is worth noting that general magneto-electric boundary conditions can be imposed, but hereafter, without lack of generality because only the through the thickness difference of the potential is usually relevant, the cases with electric and magnetic scalar potentials set to constant values at the beam bottom surface will be presented

$$\varphi^-\left(y=-\frac{h}{2}\right)=\Phi^-, \qquad \psi^-\left(y=-\frac{h}{2}\right)=\Psi^-. \quad (10)$$

It follows that four magneto-electric boundary conditions cases exist as a combinations of equations (10) and the following relationships

$$\begin{aligned}
&\textbf{(I)} \quad \varphi^+\left(y=\frac{h}{2}\right)=\Phi(x,t), \qquad \psi^+\left(y=\frac{h}{2}\right)=\Psi(x,t)\\
&\textbf{(II)} \quad D_y^+\left(y=\frac{h}{2}\right)=D_n(x,t),\\
&\qquad B_y^+\left(y=\frac{h}{2}\right)=B_n(x,t)\\
&\textbf{(III)} \quad \varphi^+\left(y=\frac{h}{2}\right)=\Phi(x,t),\\
&\qquad B_y^+\left(y=\frac{h}{2}\right)=B_n(x,t)\\
&\textbf{(IV)} \quad D_y^+\left(y=\frac{h}{2}\right)=D_n(x,t),\\
&\qquad \psi^+\left(y=\frac{h}{2}\right)=\Psi(x,t).
\end{aligned} \quad (11)$$

Equations (9) and (10) substituted into equation (7) yield

$$\begin{aligned}
a_2^+ &= \Phi^- - \left[A_\varphi^-\frac{\partial\vartheta}{\partial x}+B_\varphi^-\frac{\partial^2 v}{\partial x^2}\right]\frac{h^2}{8}+\left(Ca_1^+ + Da_3^+\right)\frac{h}{2}\\
a_4^+ &= \Psi^- - \left[A_\psi^-\frac{\partial\vartheta}{\partial x}+B_\psi^-\frac{\partial^2 v}{\partial x^2}\right]\frac{h^2}{8}+\left(Aa_1^+ + Ba_3^+\right)\frac{h}{2}
\end{aligned} \quad (12)$$

while equations (11) are used to compute the last two integration constants a_1^+ and a_3^+. To express them in a compact form let $\tilde{E}$ represent $\frac{2}{h}\Phi$ or D_n and $\tilde{H}$ stands for $\frac{2}{h}\Psi$ or B_n, depending on the magneto-electric boundary conditions applied on the bimorph top surface; by so doing one has

$$\begin{aligned}
a_1^+ &= E^i\tilde{E}+F^i\tilde{H}+L_\vartheta^i\frac{h}{2}\frac{\partial\vartheta}{\partial x}+L_v^i\frac{h}{2}\frac{\partial^2 v}{\partial x^2}\\
a_3^+ &= G^i\tilde{E}+H^i\tilde{H}+M_\vartheta^i\frac{h}{2}\frac{\partial\vartheta}{\partial x}+M_v^i\frac{h}{2}\frac{\partial^2 v}{\partial x^2}
\end{aligned} \quad (13)$$

where $E^i, F^i, G^i, H^i, L_\vartheta^i, L_v^i, M_\vartheta^i$ and M_v^i, with $i = \{\mathbf{I}, \mathbf{II}, \mathbf{III}, \mathbf{IV}\}$ according to equation (11), are combinations of material constants related to the electromagnetic behavior and to the piezoelectric and piezomagnetic characteristics as summarized in appendix B, table B.1.

Eventually, equations (7), incorporating equations (9), (12) and (13), become

$$\begin{aligned}
\varphi^\pm &= b_1^\pm(y)\frac{\partial\vartheta}{\partial x}+b_2^\pm(y)\frac{\partial^2 v}{\partial x^2}+b_3^\pm(y)\tilde{E}+b_4^\pm(y)\tilde{H}+\Phi^-\\
\psi^\pm &= b_5^\pm(y)\frac{\partial\vartheta}{\partial x}+b_6^\pm(y)\frac{\partial^2 v}{\partial x^2}+b_7^\pm(y)\tilde{E}+b_8^\pm(y)\tilde{H}+\Psi^-
\end{aligned} \quad (14)$$

where $b_n^\pm(n = 1,2,\ldots,8)$ are known functions of the transverse coordinate and are listed for the sake of completeness in appendix B from equations (B.4) to (B.7). It appears from equations (14) that both the electric and magnetic potential distributions through the bimorph thickness direction are expressed in terms of the $b_n(y)$ functions, while the variation along the beam length direction of φ and ψ directly depends on the kinematic variables. Thus, to obtain the complete analytic expressions for the magneto-electric variables involved in the analysis, the equations of motion solution is needed.

3.2. Mechanical problem

The magneto-electro-elastic bimorph beam equilibrium equations in terms of the bending moment M and the shear force T, taking into account both the translational and rotational inertia, are

$$\frac{\partial T}{\partial x}+q_0=\rho h\frac{\partial^2 v}{\partial t^2} \qquad \frac{\partial M}{\partial x}+T+m_0=\rho\frac{h^3}{12}\frac{\partial^2\vartheta}{\partial t^2} \quad (15)$$

where q_0 and m_0 are the external transverse force and bending moment per unit length applied on the beam, respectively, while ρ is the beam mass per unit volume. Taking into account the constitutive relationships equations (5), the gradient relationships equations (3) and (4) and the electric and magnetic potential functions equation (14) one has

$$T=\int_{-\frac{h}{2}}^{\frac{h}{2}}\sigma_{xy}\,\mathrm{d}y=S\left(\frac{\partial v}{\partial x}-\vartheta\right) \quad (16)$$

$$M=\int_{-\frac{h}{2}}^{\frac{h}{2}}\sigma_{xx}\,y\,\mathrm{d}y=K_\vartheta\frac{\partial\vartheta}{\partial x}+K_v\frac{\partial^2 v}{\partial x^2}+P_E\tilde{E}+P_H\tilde{H} \quad (17)$$

where S is the bimorph shear stiffness, K_ϑ is the magneto-electro-elastic equivalent bending stiffness of the bimorph beam while K_v is an additional bending stiffness related to the second derivative of the transverse displacement that is present when piezoelectric or piezomagnetic coupling exists. The equivalent beam stiffness constants, with κ being the shear factor, read as follows

$$S=\kappa(c_{44}^+ + c_{44}^-)\frac{h}{2} \quad (18)$$

$$\begin{aligned}
K_\vartheta = \frac{h^3}{24}\big[&(c^+ + c^-)-(e^-A_\varphi^- + e^+A_\varphi^+)-(d^-A_\psi^- + d^+A_\psi^+)\\
&+\tfrac{3}{2}L_\vartheta^i(e^-C - e^+ + d^-A)+\tfrac{3}{2}M_\vartheta^i(e^-D - d^+ + d^-B)\big]
\end{aligned} \quad (19)$$

$$\begin{aligned}
K_v = \frac{h^3}{24}\big[&-(e^-B_\varphi^- + e^+B_\varphi^+)-(d^-B_\psi^- + d^+B_\psi^+)\\
&+\tfrac{3}{2}L_v^i(e^-C - e^+ + d^-A)+\tfrac{3}{2}M_v^i(e^-D - d^+ + d^-B)\big].
\end{aligned} \quad (20)$$

P_E and P_H in equation (17) are representative of the bimorph beam piezoelectric and piezomagnetic constants and are defined as

$$P_E = \frac{h^2}{8}[E^i(e^-C - e^+ + d^-A) + G^i(e^-D - d^+ + d^-B)] \tag{21}$$

$$P_H = \frac{h^2}{8}[F^i(e^-C - e^+ + d^-A) + H^i(e^-D - d^+ + d^-B)]. \tag{22}$$

By using equations (16) and (17) in equation (15), the magneto-electro-elastic bimorph equations of motion can be rewritten in terms of kinematical variables only as

$$\begin{aligned} &S\frac{\partial^2 v}{\partial x^2} - S\frac{\partial \vartheta}{\partial x} + q_0 = \rho h \frac{\partial^2 v}{\partial t^2} \\ &K_\vartheta \frac{\partial^2 \vartheta}{\partial x^2} + K_v \frac{\partial^3 v}{\partial x^3} + S\frac{\partial v}{\partial x} - S\vartheta + m_0 + P_E \frac{\partial \tilde{E}}{\partial x} \\ &\quad + P_H \frac{\partial \tilde{H}}{\partial x} = \rho \frac{h^3}{12}\frac{\partial^2 \vartheta}{\partial t^2}. \end{aligned} \tag{23}$$

Equations (23) together with the boundary and initial conditions constitute the magneto-electro-elastic bimorph beam governing equations.

4. Natural frequencies and mode shapes

The free vibrations problem, specified by the homogeneous differential equation of motion and homogeneous boundary conditions, is first considered. Let us assume that the solution to the free vibration governing equations, obtained from equations (23) by forcing q_0 and m_0 to zero, can be written in the form

$$v(x,t) = V_n(x)\mathrm{e}^{\mathrm{j}\omega_n t} \qquad \vartheta(x,t) = \Theta_n(x)\mathrm{e}^{\mathrm{j}\omega_n t} \tag{24}$$

where V_n and Θ_n are the mode shapes associated with the natural circular frequency ω_n and $\mathrm{j} = \sqrt{-1}$. By virtue of equations (24), the homogeneous differential equations of motion lead to

$$\begin{aligned} &SV_n'' - S\Theta_n' + \rho h\omega_n^2 V_n = 0 \\ &K_\vartheta \Theta_n'' + K_v V_n''' + SV_n' - S\Theta_n + \rho\frac{h^3}{12}\omega_n^2\Theta_n = 0 \end{aligned} \tag{25}$$

where the prime denotes differentiation with respect to x. In order to determine the natural frequencies and the eigenfunctions, the generic mode shape is written as

$$\begin{bmatrix} V_n \\ \Theta_n \end{bmatrix} = \begin{bmatrix} C^i_{V_n} \\ C^i_{\Theta_n} \end{bmatrix} \mathrm{e}^{\lambda_{ni}x} \qquad i = \{1,2,3,4\} \tag{26}$$

and from the system of differential equations of equations (25) it follows that

$$\begin{bmatrix} S\lambda_{ni}^2 + \rho h\omega_n^2 & -S\lambda_{ni} \\ (K_v\lambda_{ni}^2 + S)\lambda_{ni} & K_\vartheta\lambda_{ni}^2 - S + \frac{\rho h^3}{12}\omega_n^2 \end{bmatrix} \begin{bmatrix} C^i_{V_n} \\ C^i_{\Theta_n} \end{bmatrix} = \begin{bmatrix} 0 \\ 0 \end{bmatrix}. \tag{27}$$

Thus, a non-trivial solution implies the determinant of the coefficients matrix of equation (27) becomes zero, i.e.

$$(K_\vartheta + K_v)\lambda_n^4 + \rho h\left(\frac{h^2}{12} + \frac{K_\vartheta}{S}\right)\omega_n^2\lambda_n^2 + \rho h\left(\frac{\rho h^3}{12S}\omega_n^2 - 1\right)\omega_n^2 = 0. \tag{28}$$

It is worth noting that the solution of equation (28) depends on the frequency ω_n; in particular it is found that

(i) if $\omega_n^2 < 12S/\rho h^3$, the roots of the characteristic equation can be denoted as $\pm\alpha_n(\omega_n)$ and $\pm\mathrm{j}\beta_n(\omega_n)$ and the general mode shape is

$$\begin{aligned} \begin{bmatrix} V_n \\ \Theta_n \end{bmatrix} &= C_{1n}\begin{bmatrix} \sinh\alpha_n x \\ \frac{\alpha_n^2 + \frac{\rho h}{S}\omega_n^2}{\alpha_n}\cosh\alpha_n x \end{bmatrix} \\ &\quad + C_{2n}\begin{bmatrix} \cosh\alpha_n x \\ \frac{\alpha_n^2 + \frac{\rho h}{S}\omega_n^2}{-\alpha_n}\sinh\alpha_n x \end{bmatrix} \\ &\quad + C_{3n}\begin{bmatrix} \sin\beta_n x \\ \frac{-\beta_n^2 + \frac{\rho h}{S}\omega_n^2}{-\beta_n}\cos\beta_n x \end{bmatrix} \\ &\quad + C_{4n}\begin{bmatrix} \cos\beta_n x \\ \frac{-\beta_n^2 + \frac{\rho h}{S}\omega_n^2}{\beta_n}\sin\beta_n x \end{bmatrix}, \end{aligned} \tag{29}$$

(ii) if $\omega_n^2 = 12S/\rho h^3$, the characteristic equation admits 0 as a solution with multiplicity 2 and $\pm\mathrm{j}\beta(\omega_n)$ as the other two roots. In this case, the mode shape is

$$\begin{aligned} \begin{bmatrix} V_n \\ \Theta_n \end{bmatrix} &= C_{1n}\begin{bmatrix} 0 \\ 1 \end{bmatrix} + C_{2n}\begin{bmatrix} 1 \\ \frac{12}{h^2}x \end{bmatrix} \\ &\quad + C_{3n}\begin{bmatrix} \sin\beta_n x \\ \frac{\frac{12}{h^2} - \beta_n^2}{-\beta_n}\cos\beta_n x \end{bmatrix} + C_{4n}\begin{bmatrix} \cos\beta_n x \\ \frac{\frac{12}{h^2} - \beta_n^2}{\beta_n}\sin\beta_n x \end{bmatrix}, \end{aligned} \tag{30}$$

(iii) if $\omega_n^2 > 12S/\rho h^3$, the roots of the characteristic equation can be denoted as $\pm\mathrm{j}\gamma(\omega_n)$ and $\pm\mathrm{j}\beta(\omega_n)$ and the general eigenfunction is

$$\begin{aligned} \begin{bmatrix} V_n \\ \Theta_n \end{bmatrix} &= C_{1n}\begin{bmatrix} \sin\gamma_n x \\ \frac{-\gamma_n^2 + \frac{\rho h}{S}\omega_n^2}{-\gamma_n}\cos\gamma_n x \end{bmatrix} \\ &\quad + C_{2n}\begin{bmatrix} \cos\gamma_n x \\ \frac{-\gamma_n^2 + \frac{\rho h}{S}\omega_n^2}{\gamma_n}\sin\gamma_n x \end{bmatrix} \\ &\quad + C_{3n}\begin{bmatrix} \sin\beta_n x \\ \frac{-\beta_n^2 + \frac{\rho h}{S}\omega_n^2}{-\beta_n}\cos\beta_n x \end{bmatrix} \\ &\quad + C_{4n}\begin{bmatrix} \cos\beta_n x \\ \frac{-\beta_n^2 + \frac{\rho h}{S}\omega_n^2}{\beta_n}\sin\beta_n x \end{bmatrix}. \end{aligned} \tag{31}$$

Since the roots of equation (28) are functions of ω_n, the boundary conditions at both ends of the beam are to be taken into account in order to determine the natural frequencies. Three distinct boundary conditions are considered in the present work, namely the simply supported beam, denoted by S–S, the clamped-free beam denoted as C–F and the clamped–clamped configuration denoted as C–C. In particular, for each of the boundary configurations one has

$$\begin{aligned} &\text{S–S}: \quad V(0) = M(0) = V(L) = M(L) = 0 \\ &\text{C–F}: \quad V(0) = \Theta(0) = T(L) = M(L) = 0 \\ &\text{C–C}: \quad V(0) = \Theta(0) = V(L) = \Theta(L) = 0. \end{aligned} \tag{32}$$

It must be highlighted that for the magneto-electro-elastic bimorph beam, differently from the mechanical Timoshenko beam, the homogeneous boundary conditions for the bending moment do not imply that the cross sectional rotation derivative is set to zero. In fact, recalling equation (17), it is easily seen that the homogeneous boundary conditions for the kinematical variables are obtained if, and only if, the magneto-electric

boundary conditions on both the top and bottom surfaces of the bimorph are homogeneous too. Thus, by imposing homogeneous mechanical and magneto-electric boundary conditions, a homogeneous system of algebraic equations is obtained, whose coefficient matrix eigenvalues, ω_n, represent the magneto-electro-elastic bimorph beam natural frequencies. Once the eigenvectors are computed for each natural frequency, the mode shapes, equations (29), (30) or (31), are determined in terms of an amplification factor only.

5. Forced vibrations solution

The forced vibrations problem of the magneto-electro-elastic beam is characterized by the existence of three kinds of loads. Besides the mechanical loads, such as distributed or concentrated forces or bending moments, the beam can experience electric or magnetic loads. Application of the magneto-electric boundary conditions equations (11) allows us to model the presence of through the thickness electric or magnetic fields. The influence of the electric and/or magnetic loads on the lateral vibration behavior is analytically introduced in the forced vibration problem by the bending moment equation (17). Moreover, it is worth noting that the electric and magnetic loads can enter the transverse vibration problem as time-dependent boundary conditions. In fact, differently from the elastic beam where the zero bending moment boundary condition directly implies a stationary condition on the kinematical variable, in the case of the magneto-electro-elastic beam the related kinematical variables result to be constrained in such a way to undergo a bending moment which varies with time. Thus, to take into account the mechanical and the electromagnetic loads, the problem of forced vibration is solved by extending the procedure proposed by Mindlin and Goodman [40] to deal with time-dependent boundary conditions for a Euler–Bernoulli beam. The procedure has then been applied to the Timoshenko beam by Hermann [43] and, for the sake of completeness, is here presented for the magneto-electro-elastic Timoshenko bimorph beam. The main idea behind the Mindlin and Goodman procedure is to take full advantage of the property of orthogonality of the principal mode of free vibration and to make use of the classical method of separation of variables by seeking the particular solution of the equation of motion equations (23) in a form that allows us to reduce the forced vibration problem to a free vibration problem and integration of polynomial functions.

The property of orthogonality of the principal modes of vibration is written, in matrix form, as

$$\int_0^L \left(\mathbf{V}^{\mathrm{T}}\mathbf{V} + \frac{h^2}{12}\boldsymbol{\Theta}^{\mathrm{T}}\boldsymbol{\Theta}\right) \mathrm{d}x = \mathbf{L} \tag{33}$$

being $\mathbf{L}(i, j) = 0$ if $i \neq j$, and

$$\begin{aligned} \mathbf{V}(x) &= [V_1(x), V_2(x), \ldots, V_n(x), \ldots, V_\infty(x)] \\ \boldsymbol{\Theta}(x) &= [\Theta_1(x), \Theta_2(x), \ldots, \Theta_n(x), \ldots, \Theta_\infty(x)]\,. \end{aligned} \tag{34}$$

Table 1. Time-dependent boundary conditions notation.

$f_1(t)$	$v(t)$ or $T(t)$	at $x = 0$
$f_2(t)$	$\vartheta(t)$ or $M(t)$, $\tilde{E}(t)$, $\tilde{H}(t)$	at $x = 0$
$f_3(t)$	$v(t)$ or $T(t)$	at $x = L$
$f_4(t)$	$\vartheta(t)$ or $M(t)$, $\tilde{E}(t)$, $\tilde{H}(t)$	at $x = L$

The particular solution is sought in the form

$$\begin{aligned} v(x,t) &= w(x,t) + \sum_{i=1}^{4} g_{iv}(x) f_i(t) \\ \vartheta(x,t) &= \beta(x,t) + \sum_{i=1}^{4} g_{i\vartheta}(x) f_i(t) \end{aligned} \tag{35}$$

where g_{iv} and $g_{i\vartheta}$ are functions chosen in such a way to ensure homogeneous boundary conditions for the functions w and β. In equations (35) f_i are representative of the time-varying boundary conditions as shown in table 1.

Once the functions g_{iv} and $g_{i\vartheta}$ are determined for a given set of time-varying boundary conditions, the remaining problem is to solve the equation of motion in terms of the functions $w(x,t)$ and $\beta(x,t)$. By substituting equations (35) into (23), the governing equations for $w(x,t)$ and $\beta(x,t)$ are obtained

$$\begin{aligned} &S\left(\frac{\partial\beta}{\partial x} - \frac{\partial^2 w}{\partial x^2}\right) + \rho h \frac{\partial^2 w}{\partial t^2} \\ &\quad = q_0 + \sum_{i=1}^{4} S\left(g_{iv}'' - g_{i\vartheta}'\right) f_i(t) - \sum_{i=1}^{4} \rho h g_{iv} \ddot{f}_i(t) \end{aligned} \tag{36}$$

$$\begin{aligned} &-K_\vartheta \frac{\partial^2\beta}{\partial x^2} - K_v \frac{\partial^3 w}{\partial x^3} + S\left(\beta - \frac{\partial w}{\partial x}\right) + \rho \frac{h^3}{12}\frac{\partial^2\beta}{\partial t^2} \\ &\quad = m_0 + P_E \frac{\partial\tilde{E}}{\partial x} + P_H \frac{\partial\tilde{H}}{\partial x} \\ &\qquad + \sum_{i=1}^{4}\left[K_\vartheta g_{i\vartheta}'' + K_v g_{iv}''' + S\left(g_{iv}' - g_{i\vartheta}\right)\right] f_i(t) \\ &\qquad - \sum_{i=1}^{4} \rho \frac{h^3}{12} g_{i\vartheta} \ddot{f}_i(t) \end{aligned} \tag{37}$$

while the initial conditions, by using equation (35), are written as

$$\begin{aligned} w(x,0) &= v(x,0) - \sum_{i=1}^{4} g_{iv}(x) f_i(0) \\ \beta(x,0) &= \vartheta(x,0) - \sum_{i=1}^{4} g_{i\vartheta}(x) f_i(0) \\ \dot{w}(x,0) &= \dot{v}(x,0) - \sum_{i=1}^{4} g_{iv}(x) \dot{f}_i(0) \\ \dot{\beta}(x,0) &= \dot{\vartheta}(x,0) - \sum_{i=1}^{4} g_{i\vartheta}(x) \dot{f}_i(0) \end{aligned} \tag{38}$$

where dots indicate differentiation with respect to time.

In order to solve equations (36) and (37), the functions $w(x,t)$ and $\beta(x,t)$ are written as a superposition of the

Table 2. Frequencies (Hz) for the piezoelectric beam. (Note: ( ) computed by using Ansys® multiphysics [33], [ ] computed by using the magneto-electro-elastic FE [33].)

	Mode	C–C		C–F		S–S	
	1	1056.3	(1058.4)	170.81	(170.83)	477.3	(476.4)
Plane	2	2801.0	(2807.0)	1047.3	(1047.5)	1864.3	(1859.9)
Stress	3	5239.4	(5252.3)	2837.9	(2839.2)	*3980.3*	(*3490.6*)
State	4	*7960.6*	(*7975.1*)	*3980.3*	(*3980.9*)	4043.7	(4031.0)
	5	8214.8	(8238.4)	5324.0	(5328.7)	6864.7	(6836.4)
	1	1021.3	[1042.34]	164.8	[167.17]	460.9	[467.38]
Monoaxial	2	2715.6	[2783.21]	1011.9	[1029.73]	1805.5	[1835.7]
Stress	3	5095.6	[5267.51]	2748.2	[2809.58]	*3839.6*	[*3573.48*]
State	4	*7679.2*	[*7689.42*]	*3839.6*	[*3841.22*]	3932.9	[4014.79]
	5	8015.9	[8333.28]	5170.9	[5317.97]	6710.2	[6883.36]

previously determined natural mode shapes as follows

$$w(x,t) = \mathbf{V}(x)\mathbf{t}(t) \qquad \beta(x,t) = \mathbf{\Theta}(x)\mathbf{t}(t) \tag{39}$$

and the right-hand side of both equations is expanded in a series of functions $\mathbf{V}(x)$ and $\mathbf{\Theta}(x)$ in order to determine the mode shapes amplification factors $\mathbf{t}(t)$. In particular, following Hermann [43], the last terms of the right-hand side of equations (36) and (37) can be expanded as

$$g_{iv} = \mathbf{V}\mathbf{G}_i \qquad g_{i\vartheta} = \mathbf{\Theta}\mathbf{G}_i \tag{40}$$

where

$$\mathbf{G}_i^{\mathrm{T}} = [G_{i1}, G_{i2}, \ldots, G_{in}, \ldots, G_{i\infty}]. \tag{41}$$

The terms of equations (36) and (37) multiplying $f_i(t)$ are expanded as

$$\begin{gathered} \frac{S}{\rho h}\left(g_{iv}'' - g_{i\vartheta}'\right) = \mathbf{V}\mathbf{G}_i^* \\ \frac{12}{\rho h^3}\left[K_\vartheta g_{i\vartheta}'' + K_v g_{iv}''' + S\left(g_{iv}' - g_{i\vartheta}\right)\right] = \mathbf{\Theta}\mathbf{G}_i^* \end{gathered} \tag{42}$$

while the applied time-dependent loads are written as

$$\begin{gathered} \frac{q_0}{\rho h} = \mathbf{V}\mathbf{Q} \\ \frac{12}{\rho h^3}\left[m_0 + P_E\frac{\partial \tilde{E}}{\partial x} + P_H\frac{\partial \tilde{H}}{\partial x}\right] = \mathbf{\Theta}\mathbf{Q} \end{gathered} \tag{43}$$

having $\mathbf{G}_i^*$ and $\mathbf{Q}$ in the same form as equation (41). By virtue of the orthogonality condition equation (33), the series coefficients $\mathbf{G}_i$, $\mathbf{G}_i^*$ and $\mathbf{Q}$ read as

$$\begin{aligned} \mathbf{G}_i &= \mathbf{L}^{-1}\int_0^L \left(\mathbf{V}^{\mathrm{T}} g_{iv} + \frac{h^2}{12}\mathbf{\Theta}^{\mathrm{T}} g_{i\vartheta}\right) \mathrm{d}x \\ \mathbf{G}_i^* &= \frac{S}{\rho h}\mathbf{L}^{-1}\int_0^L \left[\mathbf{V}^{\mathrm{T}}\left(g_{iv}'' - g_{i\vartheta}'\right)\right. \\ &\quad \left. + \mathbf{\Theta}^{\mathrm{T}}\left(\frac{K_\vartheta}{S} g_{i\vartheta}'' + \frac{K_v}{S} g_{iv}''' + g_{iv}' - g_{i\vartheta}\right)\right] \mathrm{d}x \\ \mathbf{Q} &= \frac{1}{\rho h}\mathbf{L}^{-1}\int_0^L \left[\mathbf{V}^{\mathrm{T}} q_0 + \mathbf{\Theta}^{\mathrm{T}}\left(m_0 + P_E\frac{\partial \tilde{E}}{\partial x} + P_H\frac{\partial \tilde{H}}{\partial x}\right)\right] \mathrm{d}x. \end{aligned} \tag{44}$$

Thus, by using equations (39)–(43) in equations (36) and (37) and by taking into account equations (25), the following relationships are obtained

$$\begin{aligned} \mathbf{V}\left[\ddot{\mathbf{t}} + \mathbf{\Omega}\mathbf{t} - \mathbf{Q} - \sum_{i=1}^{4}\mathbf{G}_i^* f_i + \sum_{i=1}^{4}\mathbf{G}_i \ddot{f}_i\right] &= \mathbf{0} \\ \mathbf{\Theta}\left[\ddot{\mathbf{t}} + \mathbf{\Omega}\mathbf{t} - \mathbf{Q} - \sum_{i=1}^{4}\mathbf{G}_i^* f_i + \sum_{i=1}^{4}\mathbf{G}_i \ddot{f}_i\right] &= \mathbf{0} \end{aligned} \tag{45}$$

where $\mathbf{\Omega}$ is a diagonal matrix such as $\mathbf{\Omega}(n,n) = \omega_n^2$. By integrating over the beam length the sum of the first of equations (45) multiplied by $\mathbf{V}^{\mathrm{T}}$ and the second of equations (45) multiplied by $\frac{h^2}{12}\mathbf{\Theta}^{\mathrm{T}}$, in view of the orthogonality condition equation (33), the following set of ordinary uncoupled differential equations on $\mathbf{t}$, solvable by a standard procedure, is obtained

$$\ddot{\mathbf{t}} + \mathbf{\Omega}\mathbf{t} = \mathbf{Q} + \sum_{i=1}^{4}\mathbf{G}_i^* f_i - \sum_{i=1}^{4}\mathbf{G}_i \ddot{f}_i. \tag{46}$$

The solution of equation (46) represents the mode shapes amplification factors that allow us to write the problem solution in terms of the beam mean-line transverse displacement and of the cross sectional rotation by virtue of equations (39) and (35).

6. Verifications and applications

6.1. Free vibration

Some results are presented to assess the reliability and effectiveness of the proposed model. In the first application, the eigenfrequencies of a single layer piezoelectric beam are computed for different boundary conditions, see table 2, and compared to those calculated by Annigeri *et al* [33] by using Ansys® multiphysics and the finite element formulation developed for a magneto-electro-elastic in-plane plate element. $BaTiO_3$ piezoelectric material constants are listed in table 3, the material density is $\rho = 5800\ \mathrm{kg\,m^{-3}}$ while the beam dimensions are $L = 0.3$ m and $h = 0.02$ m.

The second example considered is a homogeneous beam made of the particulate magneto-electro-elastic composite, namely BF60, with a 60% volume fraction of $BaTiO_3$ and a 40% volume fraction of $CoFe_2O_4$, whose material

Table 3. $BaTiO_3$ material constants.

C_{ij} (10^9 Pa)	ε_{ij} (10^{-9} F m^{-1})	μ_{ij} (10^{-6} N s^2 C^{-2})	e_{ij} (C m^{-2})	d_{ij} (N A m^{-1})	η_{ij} (10^{-12} N s V^{-1} C^{-1})
$C_{11} = 166$	$\varepsilon_{11} = 11.2$	$\mu_{11} = 5$	$e_{21} = -4.4$	$d_{21} = 0$	$\eta_{11} = 0$
$C_{22} = 162$	$\varepsilon_{22} = 12.6$	$\mu_{11} = 10$	$e_{22} = 18.6$	$d_{22} = 0$	$\eta_{22} = 0$
$C_{12} = 78$			$e_{14} = 11.6$	$d_{14} = 0$	
$C_{13} = 77$					
$C_{44} = 43$					

Table 4. BF60 material constants.

C_{ij} (10^9 Pa)	ε_{ij} (10^{-9} F m^{-1})	μ_{ij} (10^{-6} N s^2 C^{-2})	e_{ij} (C m^{-2})	d_{ij} (N A m^{-1})	η_{ij} (10^{-12} N s V^{-1} C^{-1})
$C_{11} = 200$	$\varepsilon_{11} = 0.9$	$\mu_{11} = -150$	$e_{21} = -3.5$	$d_{21} = 200$	$\eta_{11} = 6$
$C_{22} = 190$	$\varepsilon_{22} = 7.5$	$\mu_{11} = 75$	$e_{22} = 11$	$d_{22} = 260$	$\eta_{22} = 2500$
$C_{12} = 110$			$e_{14} = 0$	$d_{14} = 180$	
$C_{13} = 110$					
$C_{44} = 45$					

Table 5. Frequencies (Hz) for the BF60 beam. (Note: ( ) FEM results [33].)

Mode	C–C		C–F		S–S	
1	1053.70	(1054.93)	169.96	(169.97)	475.41	(474.67)
2	2800.24	(2805.75)	1043.3	(1043.76)	1861.03	(1858.33)
3	5250.08	(5266.99)	2831.8	(2835.36)	*3961.14*	(*3632.54*)
4	*7922.28*	(*7812.88*)	*3959.4*	(*3902.01*)	4049.69	(4045.01)
5	8250.11	(8291.21)	5323.2	(5337.23)	6900.88	(6896.23)
6	11 675.43	(11 758.60)	8385.6	(8423.05)	10 272.44	(10 274.55)
7	15 423.76	(15 572.90)	*11 878.0*	(*11 704.94*)	*11 883.43*	(*10 918.21*)
8	*15 844.57*	(*15 623.80*)	11 887.3	(11 967.14)	14 039.43	(14 056.89)
9	19 416.33	(19 659.70)	15 720.6	(15 867.42)	18 100.68	(18 150.64)
10	23 593.71	(23 430.00)	*19 796.7*	(*19 504.23*)	*19 805.71*	(*18 256.71*)

Table 6. $CoFe_2O_4$ material constants.

C_{ij} (10^9 Pa)	ε_{ij} (10^{-9} F m^{-1})	μ_{ij} (10^{-6} N s^2 C^{-2})	e_{ij} (C m^{-2})	d_{ij} (N A m^{-1})	η_{ij} (10^{-12} N s V^{-1} C^{-1})
$C_{11} = 286$	$\varepsilon_{11} = 0.08$	$\mu_{11} = -590$	$e_{21} = 0$	$d_{21} = 580.3$	$\eta_{11} = 0$
$C_{22} = 269.5$	$\varepsilon_{22} = 0.093$	$\mu_{22} = 157$	$e_{22} = 0$	$d_{22} = 699.7$	$\eta_{22} = 0$
$C_{12} = 170.5$			$e_{14} = 0$	$d_{14} = 550$	
$C_{13} = 173$					
$C_{44} = 45.3$					

constants [33, 16] are shown in table 4, while the volume density has been computed to be 5550 kg m^{-3}. The natural frequencies computed for the three boundary conditions equations (32) are listed in table 5 in comparison with the FEM analysis results [33].

The free vibration behavior of a magneto-electro-elastic laminated beam is also investigated. The beam is realized by stacking a piezoelectric $BaTiO_3$ and a piezomagnetic $CoFe_2O_4$ layer. The material constants are listed in tables 3 and 6, the overall dimensions are the same as in the previous applications while the thickness of both laminae is $h/2$. The stacking sequence appears to have no influence on the natural frequencies, that are listed in table 7, in comparison with the finite element calculation [33].

It is worth noting that in tables 2, 5 and 7, the values in italic have been found to be axial mode and that the relative natural frequencies have been computed by virtue of the free longitudinal vibrations theory, see [39] for more details, and by defining an equivalent Young's modulus for the magneto-electro-elastic beam as

$$\widehat{E} = \frac{12(K_\vartheta + K_v)}{\rho h^3}. \tag{47}$$

6.2. Forced vibration

A simply supported $CoFe_2O_4/BaTiO_3$ laminated beam is firstly studied. The beam length is $L = 0.3$ m and the overall thickness is $h = 0.02$ m. The beam undergoes a uniformly quasi-static distributed load $q = 1 - \exp(-t/0.15)$ N m^{-1}, while the electric and magnetic potentials at the beam top surface are set to zero. The material constants are listed in tables 3 and 6 for the piezoelectric and piezomagnetic layers, respectively. In order to check the proposed analytical solution, a boundary element analysis of the bimorph beam has been carried out by using the multidomain BEM presented in [36]. To compare the analytical and numerical results, the response of the beam has been studied in terms of vertical displacement, and electric and magnetic potentials at the interface point

Table 7. Frequencies (Hz) for the $BaTiO_3/CoFe_2O_4$ layered beam. (Note: ( ) FEM results [33].)

Mode	C–C		C–F		S–S	
1	1167.56	(1165.07)	189.63	(188.70)	529.80	(526.29)
2	3080.24	(3078.60)	1159.42	(1154.65)	2065.44	(2052.71)
3	5730.43	(5738.67)	3129.14	(3120.80)	*4420.84*	(*4008.32*)
4	*8841.68*	(*8683.41*)	*4420.84*	(*4335.11*)	4467.87	(4444.36)
5	8935.91	(8971.57)	5841.67	(5838.36)	7561.09	(7529.14)
6	12 555.58	(12 640.40)	9136.27	(9154.66)	11 174.64	(11 146.30)
7	16 479.50	(16 643.20)	12 861.96	(12 924.90)	*13 262.52*	(*12 053.30*)
8	*17 683.36*	(*17 358.00*)	*13 262.52*	(*13 001.50*)	15 165.55	(15 150.10)
9	20 626.50	(20 900.40)	16 897.13	(17 036.50)	19 423.23	(19 449.40)
10	24 937.25	(25 360.00)	21 155.73	(21 405.10)	*22 104.20*	(*20 163.40*)

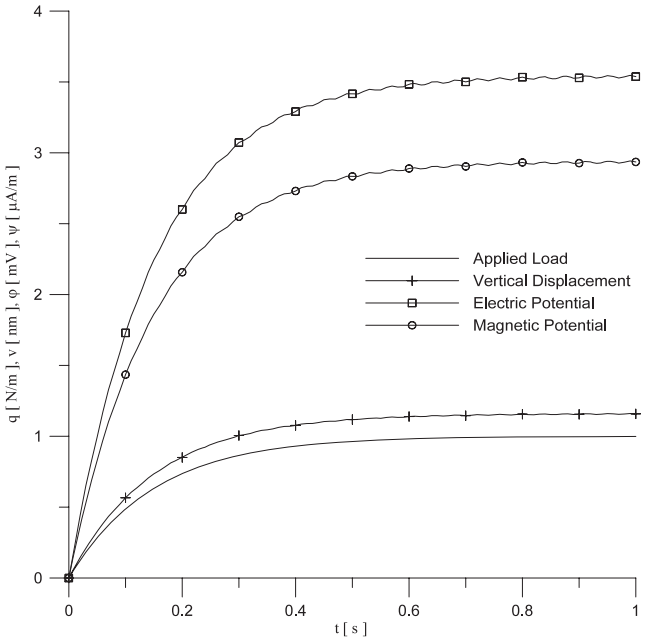

Figure 2. Applied load and magneto-electro-elastic response time history.

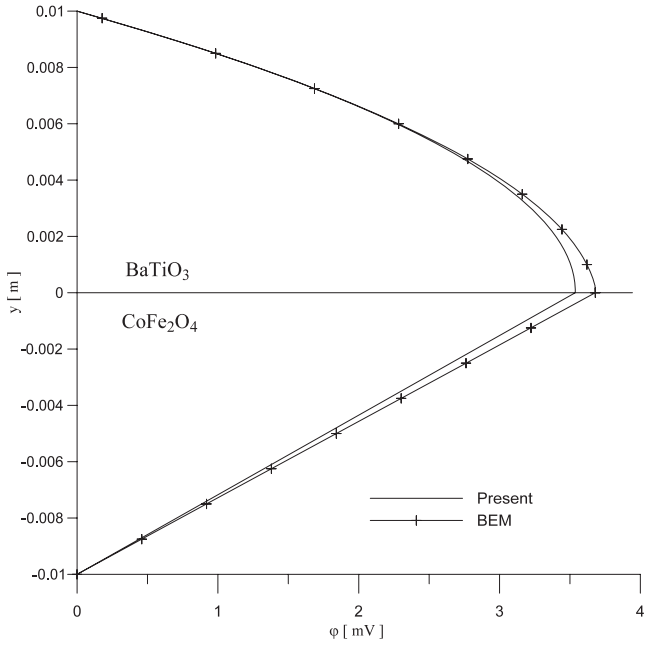

Figure 3. Steady state through the thickness electric potential distribution at $x = L/2$.

Table 8. Numerical convergence and analytical results at the point $(L/2, 0)$.

	BEM					
No elements	100	140	180	220	260	Present
v (nm)	0.806	0.972	1.051	1.093	1.114	1.158
φ (mV)	2.61	3.19	3.46	3.60	3.68	3.53
ψ (μA m^{-1})	−2.00	−2.55	−2.66	−2.75	−2.83	−2.93

$(L/2, 0)$, and good agreement has been obtained. From table 8 it appears that as the number of boundary elements increases, the numerical response tends to the analytical one. It is seen that by using 260 linear elements, the numerical solution fits quite well the analytical results with a maximum percentage discrepancy of 4% for the electric potential.

The response of the bimorph beam to the applied load is shown in figure 2. It can be observed that the vertical displacement approaches the beam's static deflection value at 0.8 s. Moreover, the behavior of both the electric and magnetic potential can be considered steady after 0.8 s even though small oscillations hold.

The through the thickness electric potential distribution at $x = L/2$ and $t = 1$ s is shown in figure 3 in comparison with the BEM results. It appears that the electric potential behaves linearly in the piezomagnetic layer and quadratically in the piezoelectric domain. A similar behavior is highlighted for the magnetic potential through the thickness distribution. The magnetic potential is a quadratic function of y in the piezomagnetic lamina while it varies linearly in the piezoelectric layer as shown in figure 4.

The second application presented deals with a clamped–clamped bimorph beam, used as an electromagnetic strain sensor, of length $L = 0.3$ m and thickness $h = 0.01$ m. The lower lamina is made by the piezomagnetic $CoFe_2O_4$ material while the upper layer medium is piezoelectric $BaTiO_3$. The material constants are listed in tables 3 and 6. The beam, at the instant $t = 0$, suddenly undergoes a sinusoidally distributed mechanical load of amplitude $q = \sin(\pi x/L)$ N m^{-1} that remains constant in time; all of the initial conditions are set to zero. The maximum transverse displacement experienced by the beam is about 3.16 nm while the electric and magnetic

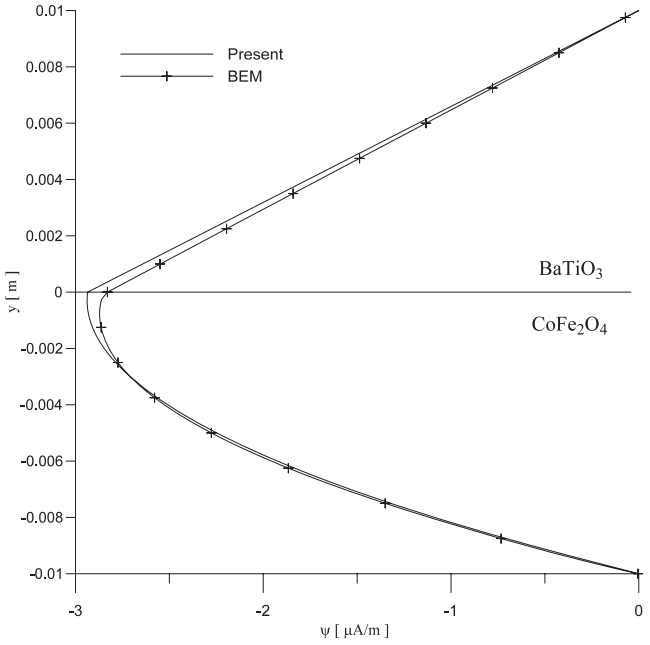

Figure 4. Steady state through the thickness magnetic potential distribution at $x = L/2$.

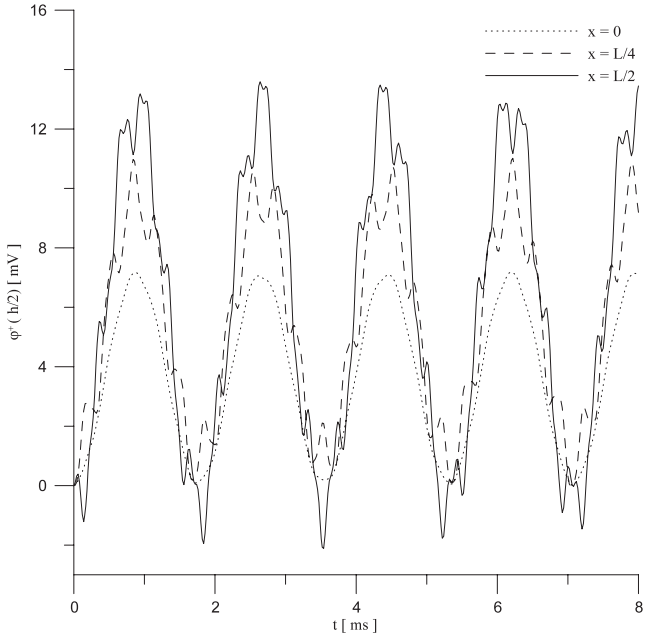

Figure 5. Electric potential on the top surface of the bimorph beam.

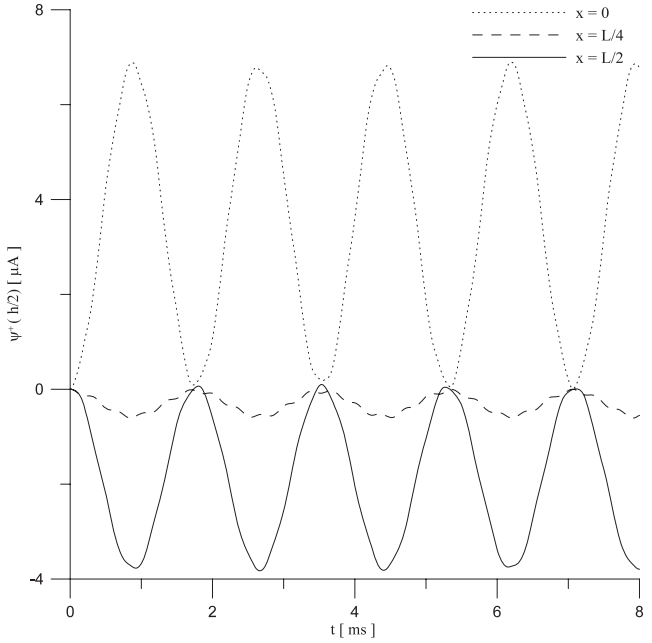

Figure 6. Magnetic potential on the top surface of the bimorph beam.

beam responses are shown in figures 5 and 6 in terms of the electric and magnetic potentials at three particular points of the bimorph top surface. From figure 6 it appears that the magnetic potential tends to oscillate at the beam's first natural frequency of 564.92 Hz; on the other hand, the electric potential is more sensitive to high frequency modes, as highlighted in figure 5. Six mode shapes were used to approximate the structure dynamic response since higher modes have been found to have a negligible influence; moreover, the functions $g_{i\theta}$ and g_{iv} are trivially zero as the boundary conditions do not depend on time.

In the third application, the proposed model is employed to simulate the behavior of a cantilever bilayer used as a magnetic field probe. The length of the beam is $L = 0.05$ m, the thickness is $h = 0.5$ mm and the lamination sequence is $CoFe_2O_4/BaTiO_3$. The magneto-electric boundary condition II, see equations (11), is used to take into account the influence of an applied magnetic induction. In particular, the applied magnetic induction is constant along the x direction, its amplitude is 10^{-5} T and varies at 2 kHz. The electric displacement on the bimorph top surface is set to zero for reading the device response corresponding to the applied magnetic load in terms of the difference of the electric potential in the beam through the thickness direction. The presence of the external magnetic induction, through the condition of zero bending moment at the free end, implies, according to table (1), the existence of the function $f_4(t)$ and, as a consequence, that the functions $g_{4\theta}$ and g_{4v} must be non-zero to assure homogeneous boundary conditions for $w(x,t)$ and $\beta(x,t)$. In particular, one has $f_4(t) = 10^{-5}\sin(4\pi 10^3 t)$, $g_{4v} = -(P_h/K_\vartheta)Lx$ and $g_{4\vartheta} = -(P_h/K_\vartheta)x$. The transverse displacement and the electric potential at the top surface of the beam at two distinct instants of time are plotted in figures (7) and (8) respectively. It appears that the beam deformation mainly affects the electric potential response mean value, whereas its distribution along the longitudinal direction tends to remain unchanged.

In figure 9, the driving magnetic load B_n, the bimorph device electric response and the beam free end displacement are compared. The graph of φ^+ shown in figure 9 is representative of the difference of the electric potential mean value along the x direction, since the electric potential at the beam bottom surface Φ^- has been set to zero. It is evident from figure 9 that the electric response of the beam varies at

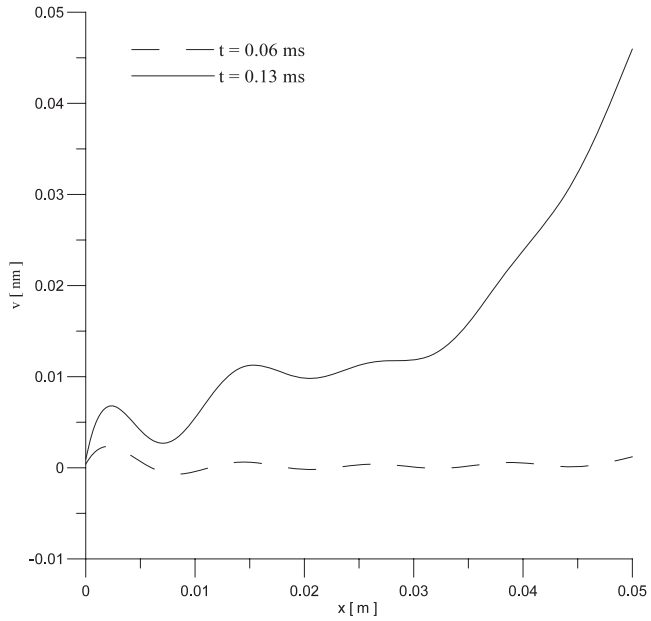

Figure 7. Snapshots of the magnetic field probe transverse displacement.

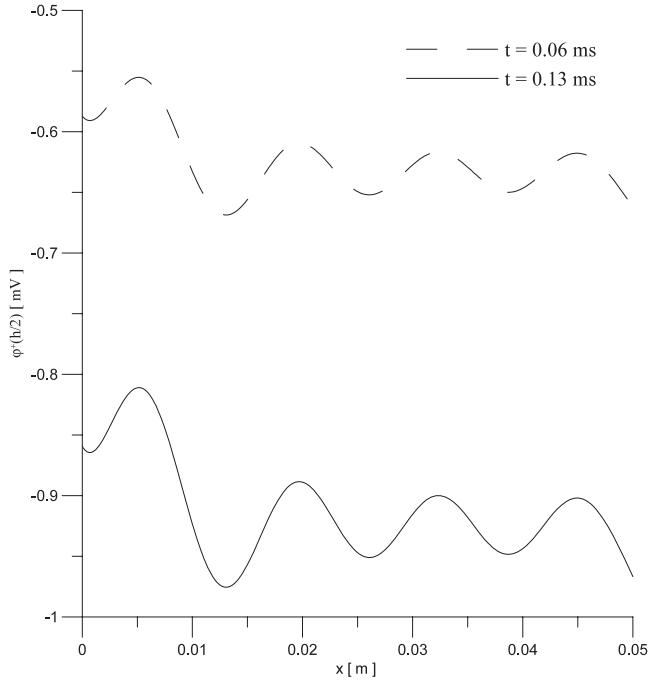

Figure 8. Snapshots of the magnetic field probe top surface electric potential distribution.

the same frequency of the applied magnetic induction, i.e. at 2 kHz; on the other hand, the beam free end oscillates at about 148.64 Hz, that is the first natural frequency of the analyzed structure.

7. Conclusions

A general analytical method for the free and forced vibration analysis of a magneto-electro-elastic bimorph beam with time-dependent boundary conditions has been presented. From the mechanical point of view, the model has been based on Timoshenko's beam theory to take into account the shear force effect. The electric and magnetic fields have been treated as quasi-static, due to the observation that the electromagnetic waves propagation velocity is several orders of magnitude higher than that of elastic waves. Moreover, the assumptions made on the electric and magnetic fields have allowed us to include the piezoelectric, piezomagnetic and electromagnetic coupling in the beam equivalent bending stiffness coefficients. The presence of an additional bending stiffness, only dependent from the piezoelectric and piezomagnetic characteristics, has been put in evidence. Moreover, it is worth pointing out that no restrictions on the magneto-electric boundary conditions have been made and that they can enter the mechanical response as an equivalent external bending moment per unit length and via the bending moment definition. Solutions for free and forced vibration problems have been obtained by means of modal expansion. Shifting functions have been used to take into account the effects of the electric and magnetic loads on the dynamic behavior of the beam, brought into the forced vibration analysis in the form of time-varying boundary conditions. As a consequence, a great variety of boundary conditions can be modeled, revealing a wide applicability of the proposed method. Free vibration analyses carried out on multiphase and laminated beams have proven the effectiveness of the proposed solution. The transient responses of magneto-electro-elastic bimorph beams employed as electromagnetic strain sensors and magnetic field probes have been obtained via the proposed method.

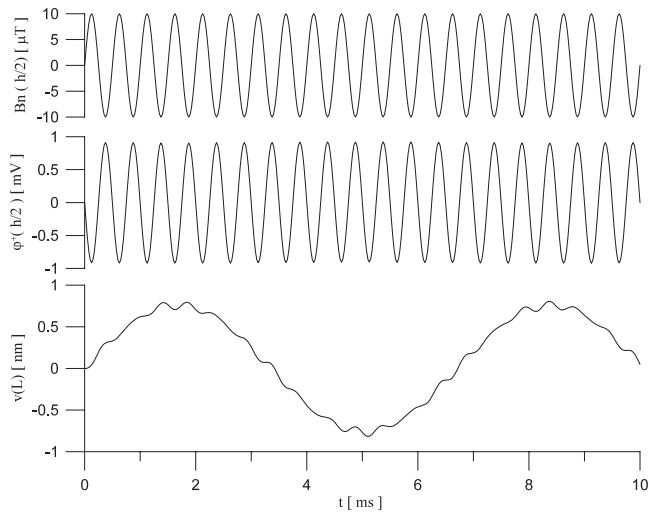

Figure 9. Applied magnetic load and electro-mechanical response of the bimorph beam.

Appendix A. Constitutive relationships and parameters

The constitutive relationships for a transversely isotropic magneto-electro-elastic composite having electric and magnetic poling directions parallel to the y-axis are obtained, by

Table B.1. Constants related to the electromagnetic top surface boundary conditions.

B.C.	I	II	III	IV
$\tilde{E}$	$\frac{2}{h}\Phi$	D_n	$\frac{2}{h}\Phi$	B_n
$\tilde{H}$	$\frac{2}{h}\Psi$	B_n	B_n	$\frac{2}{h}\Psi$
E^i	$\frac{(1+B)}{(1+C)(1+B)-AD}$	$\frac{-\mu^+}{\varepsilon^+\mu^+-\eta^{+2}}$	$\frac{-\mu^+}{\eta^+D-\mu^+(1+C)}$	$\frac{(1+B)}{\eta^+A-\varepsilon^+(1+B)}$
F^i	$\frac{-D}{(1+C)(1+B)-AD}$	$\frac{\eta^+}{\varepsilon^+\mu^+-\eta^{+2}}$	$\frac{-D}{\eta^+D-\mu^+(1+C)}$	$\frac{\eta^+}{\eta^+A-\varepsilon^+(1+B)}$
G^i	$\frac{-A}{(1+C)(1+B)-AD}$	$\frac{\eta^+}{\varepsilon^+\mu^+-\eta^{+2}}$	$\frac{\eta}{\eta^+D-\mu^+(1+C)}$	$\frac{-A}{\eta^+A-\varepsilon^+(1+B)}$
H^i	$\frac{(1+C)}{(1+C)(1+B)-AD}$	$\frac{-\varepsilon^+}{\varepsilon^+\mu^+-\eta^{+2}}$	$\frac{(1+C)}{\eta^+D-\mu^+(1+C)}$	$\frac{-\varepsilon^+}{\eta^+A-\varepsilon^+(1+B)}$
L^i_ϑ	$E^i\frac{A^-_\varphi-A^+_\varphi}{2}+F^i\frac{A^-_\psi-A^+_\psi}{2}$	$E^ic_{dv}+F^ic_{bv}$	$E^i\frac{A^-_\varphi-A^+_\varphi}{2}-F^ic_{b\vartheta}$	$-E^ic_{d\vartheta}+F^i\frac{A^-_\psi-A^+_\psi}{2}$
L^i_v	$E^i\frac{B^-_\varphi-B^+_\varphi}{2}+F^i\frac{B^-_\psi-B\psi^+}{2}$	$E^ic_{d\vartheta}+F^ic_{b\vartheta}$	$E^i\frac{B^-_\varphi-B^+_\varphi}{2}-F^ic_{bv}$	$-E^ic_{dv}+F^i\frac{B^-_\psi-B^+_\psi}{2}$
M^i_ϑ	$G^i\frac{A^-_\varphi-A^+_\varphi}{2}+H^i\frac{A^-_\psi-A^+_\psi}{2}$	$G^ic_{d\vartheta}+H^ic_{b\vartheta}$	$G^i\frac{A^-_\varphi-A^+_\varphi}{2}-H^ic_{b\vartheta}$	$-G^ic_{d\vartheta}+H^i\frac{A^-_\psi-A^+_\psi}{2}$
M^i_v	$G^i\frac{B^-_\varphi-B^+_\varphi}{2}+H^i\frac{B^-_\psi-B\psi^+}{2}$	$G^ic_{dv}+H^ic_{bv}$	$G^i\frac{B^-_\varphi-B^+_\varphi}{2}-H^ic_{bv}$	$-G^ic_{dv}+H^i\frac{B^-_\psi-B^+_\psi}{2}$

virtue of [33] and [42], and are listed, for the sake of completeness, in equation (A.1), where $C_{55}=\frac{C_{11}-C_{13}}{2}$.

$$\begin{bmatrix}\sigma_{xx}\\ \sigma_{yy}\\ \sigma_{zz}\\ \sigma_{zy}\\ \sigma_{zx}\\ \sigma_{xy}\\ D_x\\ D_y\\ D_z\\ B_x\\ B_y\\ B_z\end{bmatrix}=\begin{bmatrix} C_{11} & C_{12} & C_{13} & 0 & 0 & 0 & 0 & -e_{21}\\ C_{12} & C_{22} & C_{12} & 0 & 0 & 0 & 0 & -e_{22}\\ C_{13} & C_{12} & C_{11} & 0 & 0 & 0 & 0 & -e_{21}\\ 0 & 0 & 0 & C_{44} & 0 & 0 & 0 & 0\\ 0 & 0 & 0 & 0 & C_{55} & 0 & 0 & 0\\ 0 & 0 & 0 & 0 & 0 & C_{44} & -e_{14} & 0\\ 0 & 0 & 0 & 0 & 0 & e_{14} & \varepsilon_{11} & 0\\ e_{21} & e_{22} & e_{21} & 0 & 0 & 0 & 0 & \varepsilon_{22}\\ 0 & 0 & 0 & e_{14} & 0 & 0 & 0 & 0\\ 0 & 0 & 0 & 0 & 0 & d_{14} & \eta_{11} & 0\\ d_{21} & d_{22} & d_{21} & 0 & 0 & 0 & 0 & \eta_{22}\\ 0 & 0 & 0 & d_{14} & 0 & 0 & 0 & 0\end{bmatrix}\begin{bmatrix} 0 & 0 & -d_{21} & 0\\ 0 & 0 & -d_{22} & 0\\ 0 & 0 & -d_{21} & 0\\ -e_{14} & 0 & 0 & -d_{14}\\ 0 & 0 & 0 & 0\\ 0 & -d_{14} & 0 & 0\\ 0 & \eta_{11} & 0 & 0\\ 0 & 0 & \eta_{22} & 0\\ \varepsilon_{11} & 0 & 0 & \eta_{11}\\ 0 & \mu_{11} & 0 & 0\\ 0 & 0 & \mu_{22} & 0\\ \eta_{11} & 0 & 0 & \mu_{11}\end{bmatrix}\begin{bmatrix}\gamma_{xx}\\ \gamma_{yy}\\ \gamma_{zz}\\ \gamma_{zy}\\ \gamma_{zx}\\ \gamma_{yx}\\ E_x\\ E_y\\ E_z\\ H_x\\ H_y\\ H_z\end{bmatrix}. \quad \text{(A.1)}$$

Under the hypothesis of plane stress elasticity, some of the constitutive constants are rearranged as shown below

$$\begin{aligned}
\bar{C}_{11}&=C_{11}-\frac{C_{13}^2}{C_{11}} & \bar{C}_{12}&=C_{12}-\frac{C_{12}C_{13}}{C_{11}}\\
\bar{C}_{22}&=C_{22}-\frac{C_{12}^2}{C_{11}} & \bar{\varepsilon}_{22}&=\varepsilon_{22}+\frac{e_{21}^2}{C_{11}}\\
\bar{\eta}_{22}&=\eta_{22}+\frac{e_{21}d_{21}}{C_{11}} & \bar{\mu}_{22}&=\mu_{22}-\frac{d_{21}^2}{C_{11}}\\
\bar{e}_{21}&=e_{21}-\frac{C_{13}d_{21}}{C_{11}} & \bar{e}_{22}&=e_{22}-\frac{C_{12}e_{21}}{C_{11}}\\
\bar{d}_{21}&=d_{21}-\frac{C_{13}e_{21}}{C_{11}} & \bar{d}_{22}&=d_{22}-\frac{C_{12}d_{21}}{C_{11}}
\end{aligned} \quad \text{(A.2)}$$

while for a beam-like structure, the material parameters are

$$\begin{aligned}
c&=\bar{C}_{11}-\tilde{h}\frac{\bar{C}_{12}^2}{\bar{C}_{22}} & e&=\bar{e}_{21}-\tilde{h}\frac{\bar{C}_{12}\bar{e}_{22}}{\bar{C}_{22}}\\
d&=\bar{d}_{21}-\tilde{h}\frac{\bar{C}_{12}\bar{d}_{22}}{\bar{C}_{22}} & \varepsilon&=\bar{\varepsilon}_{22}+\tilde{h}\frac{\bar{e}_{22}^2}{\bar{C}_{22}}\\
\eta&=\bar{\eta}_{22}+\tilde{h}\frac{\bar{e}_{22}\bar{d}_{22}}{\bar{C}_{22}} & \mu&=\bar{\mu}_{22}+\tilde{h}\frac{\bar{d}_{22}^2}{\bar{C}_{22}}
\end{aligned} \quad \text{(A.3)}$$

where $\tilde{h}=0$ for plane stress analysis and $\tilde{h}=1$ for monoaxial stress analysis.

Appendix B. Magneto-electric problem constants

$$\begin{aligned}
A^\pm_\varphi&=-\frac{\mu^\pm(e^\pm_{14}+e^\pm)-\eta^\pm(d^\pm_{14}+d^\pm)}{\varepsilon^\pm\mu^\pm-\eta^{\pm2}},\\
B^\pm_\varphi&=\frac{\mu^\pm e^\pm_{14}-\eta^\pm d^\pm_{14}}{\varepsilon^\pm\mu^\pm-\eta^{\pm2}}\\
A^\pm_\psi&=-\frac{\varepsilon^\pm(d^\pm_{14}+d^\pm)-\eta^\pm(e^\pm_{14}+e^\pm)}{\varepsilon^\pm\mu^\pm-\eta^{\pm2}},\\
B^\pm_\psi&=\frac{\varepsilon^\pm d^\pm_{14}-\eta^\pm e^\pm_{14}}{\varepsilon^\pm\mu^\pm-\eta^{\pm2}}
\end{aligned} \quad \text{(B.1)}$$

$$A = \frac{\varepsilon^- \eta^+ - \eta^- \varepsilon^+}{\varepsilon^- \mu^- - \eta^{-2}}; \qquad B = \frac{\varepsilon^- \mu^+ - \eta^- \eta^+}{\varepsilon^- \mu^- - \eta^{-2}};$$
$$C = \frac{\mu^- \varepsilon^+ - \eta^- \eta^+}{\varepsilon^- \mu^- - \eta^{-2}}; \qquad D = \frac{\mu^- \eta^+ - \eta^- \mu^+}{\varepsilon^- \mu^- - \eta^{-2}} \tag{B.2}$$

$$c_{d\vartheta} = e^+ + \varepsilon^+ A_\varphi^+ + \eta^+ A_\psi^+ \qquad c_{dv} = \varepsilon^+ B_\varphi^+ + \eta^+ B_\psi^+$$
$$c_{b\vartheta} = d^+ + \eta^+ A_\varphi^+ + \mu^+ A_\psi^+ \qquad c_{bv} = \eta^+ B_\varphi^+ + \mu^+ B_\psi^+ \tag{B.3}$$

$$b_1^+ = A_\varphi^+ \frac{y^2}{2} - A_\varphi^- \frac{h^2}{8} + L_\vartheta^i \frac{h}{2} y + \left(L_\vartheta^i C + M_\vartheta^i D\right) \frac{h^2}{4}$$
$$b_2^+ = B_\varphi^+ \frac{y^2}{2} - B_\varphi^- \frac{h^2}{8} + L_v^i \frac{h}{2} y + \left(L_v^i C + M_v^i D\right) \frac{h^2}{4} \tag{B.4}$$
$$b_3^+ = E^i y + (E^i C + G^i D) \frac{h}{2}$$
$$b_4^+ = F^i y + (F^i C + H^i D) \frac{h}{2}$$

$$b_5^+ = A_\psi^+ \frac{y^2}{2} - A_\psi^- \frac{h^2}{8} + M_\vartheta^i \frac{h}{2} y + (L_\vartheta^i A + M_\vartheta^i B) \frac{h^2}{4}$$
$$b_6^+ = B_\psi^+ \frac{y^2}{2} - B_\psi^- \frac{h^2}{8} + M_v^i \frac{h}{2} y + (L_v^i A + M_v^i B) \frac{h^2}{4} \tag{B.5}$$
$$b_7^+ = G^i y + (E^i A + G^i B) \frac{h}{2}$$
$$b_8^+ = H^i y + (F^i A + H^i B) \frac{h}{2}$$

$$b_1^- = A_\varphi^- \left(\frac{y^2}{2} - \frac{h^2}{8}\right) + (L_\vartheta^i C + M_\vartheta^i D) \frac{h}{2} \left(\frac{h}{2} + y\right)$$
$$b_2^- = B_\varphi^- \left(\frac{y^2}{2} - \frac{h^2}{8}\right) + (L_v^i C + M_v^i D) \frac{h}{2} \left(\frac{h}{2} + y\right) \tag{B.6}$$
$$b_3^- = (E^i C + G^i D) \left(\frac{h}{2} + y\right)$$
$$b_4^- = (F^i C + H^i D) \left(\frac{h}{2} + y\right)$$

$$b_5^- = A_\psi^- \left(\frac{y^2}{2} - \frac{h^2}{8}\right) + (L_\vartheta^i A + M_\vartheta^i B) \frac{h}{2} \left(\frac{h}{2} + y\right)$$
$$b_6^- = B_\psi^- \left(\frac{y^2}{2} - \frac{h^2}{8}\right) + (L_v^i A + M_v^i B) \frac{h}{2} \left(\frac{h}{2} + y\right) \tag{B.7}$$
$$b_7^- = (E^i A + G^i B) \left(\frac{h}{2} + y\right)$$
$$b_8^- = (F^i A + H^i B) \left(\frac{h}{2} + y\right).$$

References

[1] Nan C W 1994 Magnetoelectric effect in composite of piezoelectric and piezomagnetic phases *Phys. Rev.* B **50** 6082–88

[2] Eerenstein M, Mathur N D and Scott J F 2006 Multiferroic and magnetoelectric materials *Nature* **442** 759–65

[3] Fiebig M 2005 Revival of the magnetoelectric effect *J. Phys. D: Appl. Phys.* **38** R123–52

[4] Wang J and Li X 2008 Analytical solutions for the magnetoelectric effect of multilayered magneto-electro-elastic media *Smart Mater. Struct.* **17** 045028

[5] Zhai J, Xing Z, Dong S, Li j and Viehland D 2006 Detection of pico-Tesla magnetic fields using magneto-electric sensors at room temperature *Appl. Phys. Lett.* **88** 062510

[6] Bayrashev A, Robbins W P and Ziaie B 2004 Low frequency wireless powering of microsystems using piezoelectric-magnetostrictive laminate composites *Sensors Actuators* A **114** 244–49

[7] Wu T L and Huang J H 2000 Closed form solutions for the magnetoelectric coupling coefficients in fibrous composites with piezoelectric and piezomagnetic phases *Int. J. Solids Struct.* **37** 2981–3009

[8] Zhai J, Xing Z, Dong S, Li j and Viehland D 2008 Magnetoelectric laminate composite: an overview *J. Am. Ceram. Soc.* **91** 351–8

[9] Ryu J, Priya S, Uchino K and Kim H E 2002 Magnetoelectric effect in composites of magnetostrictive and piezoelectric materials *J. Electroceram.* **8** 107–19

[10] Pettiford C, Dasgupta S, Lou J, Yoon S D and Sun N X 2007 Bias field effects on microwave frequency behavior of PZT/YIG magnetoelectric bilayer *IEEE Trans. Magn.* **43** 3343–5

[11] Wu D, Gong W, Deng H and Li M 2007 Magnetoelectric composite ceramics of nickel ferrite and lead zirconate titanate via *in situ* processing *J. Phys. B: At. Mol. Opt. Phys.* **40** 5002–4

[12] Wong W Y, Or S W, Chan H L W, Jia Y and Luo H 2007 Converse magnetoelectric effect in three-phase composites of piezoceramic, metal cap and magnet *J. Appl. Phys.* **101** 09N508

[13] Ryu J, Carazo A V, Uchino K and Kim H E 2001 Magnetoelectric properties in piezoelectric and magnetostrictive laminate composites *Japan. J. Appl. Phys.* **40** 4948–51

[14] Buchanan G R 2004 Layered versus multiphase magneto-electro-elastic composites *Composites* B **35** 413–20

[15] Li J Y and Dunn M L 1998 Micromechanics of magnetoelectroelastic composites: average field and effective behavior *J. Intell. Mater. Syst. Struct.* **9** 404–16

[16] Aboudi J 2001 Micromechanical analysis of fully coupled elctro-magneto-thermo-elastic multiphase composites *Smart Mater. Struct.* **10** 867–77

[17] Wang X and Shen Y 2002 The general solution of three-dimensional problems in magnetoelectroelastic media *Int. J. Eng. Sci.* **40** 1069–80

[18] Guan Q and He S 2005 Two-dimensional analysis of piezoelectric/piezomagnetic and elastic media *Compos. Struct.* **69** 229–37

[19] Hou P F, Ding H J and Chen J Y 2005 Green's functions for transversely isotropic magnetoelectroelastic media *Int. J. Eng. Sci.* **43** 826–58

[20] Pan E 2001 Exact solution for simply supported and multilayered magneto electro elastic plates *J. Appl. Mech.* **68** 608–18

[21] Pan E and Heyliger P R 2002 Free vibrations of simply supported and multilayered magneto-electro-elastic plates *J. Sound Vib.* **252** 429–42

[22] Pan E and Heyliger P R 2003 Exact solutions for magneto-electro-elastic laminates in cylindrical bending *Int. J. Solids Struct.* **40** 6859–76

[23] Heyliger P R, Ramirez F and Pan E 2004 Two-dimensional static fields in magnetoelectroelastic laminates *J. Intell. Mater. Syst. Struct.* **15** 689–709

[24] Pan E and Han F 2005 Exact solution for functionally graded and layered magneto-electro-elastic plates *Int. J. Eng. Sci.* **43** 321–39

[25] Huang D J, Ding H J and Chen W Q 2007 Analytical solution for functionally graded magneto-electro-elastic plane beams *Int. J. Eng. Sci.* **45** 467–85
[26] Ramirez F, Heyliger P R and Pan E 2006 Free vibration response of two-dimensional magneto-electro-elastic laminated plates *J. Sound Vib.* **292** 626–44
[27] Wang J G, Chen L F and Fang S 2003 State vector approach to analysis of multilayered magneto-electro-elastic plates *Int. J. Solids Struct.* **40** 1669–80
[28] Chen W Q, Lee K Y and Ding H J 2005 On free vibration of non-homogeneous transversely isotropic magneto-electro-elastic plates *J. Sound Vib.* **279** 237–51
[29] Chen W Q and Lee K Y 2003 Alternative state space formulations for magnetoelectric thermoelasticity with transverse isotropy and the application to bending analysis of nonhomogeneous plates *Int. J. Solids Struct.* **40** 5689–705
[30] Bhangale R K and Ganesan N 2005 Free vibration studies of simply supported nonhomogeneous functionally graded magneto-electro-elastic finite cylindrical shell *J. Sound Vib.* **288** 412–22
[31] Buchanan G R 2003 Free vibration of an infinite magneto-electro-elastic cylinder *J. Sound Vib.* **268** 413–26
[32] Lage R G, Mota Soares C M, Mota Soares C A and Reddy J N 2004 Layerwise partial mixed finite element analysis of magneto-electro-elastic plates *Comput. Struct.* **82** 1293–301
[33] Annigeri A R, Ganesan N and Swarnamani S 2007 Free vibration behaviour of multiphase and layered magneto-electro-elastic beam *J. Sound Vib.* **299** 44–63
[34] Ding H and Jiang A 2004 A boundary integral formulation and solution for 2D problems in magneto-electro-elastic media *Comput. Struct.* **82** 1599–607
[35] Ding H, Jiang A, Hou P F and Chen W Q 2005 Green's functions for two-phase transversely isotropic magneto-electro-elastic media *Eng. Anal. Bound. Elem.* **29** 551–61
[36] Milazzo A, Benedetti I and Orlando C 2006 Boundary element method for magneto-electro-elastic laminates *Comput. Model. Eng. Sci.* **15** 17–30
[37] Daví G, Milazzo A and Orlando C 2008 Boundary element analysis of magneto-electro-eleastic bimorph *Mech. Adv. Mater. Struct.* **15** 220–7
[38] Hou P F and Leung A Y T 2004 The transient responses of magneto-electro-elastic hollow cylinders *Smart Mater. Struct.* **13** 762–76
[39] Timoshenko S 1955 *Vibration Problems in Engineering* (Princeton, NJ: Van Nostrand Reinhold)
[40] Mindlin R D and Goodman L E 1950 Beam vibrations with time-dependent boundary conditions *ASME J. Appl. Mech.* **17** 377–80
[41] Benjeddou A, Trinidade M A and Ohayon R 2000 Piezoelectric actuation mechanisms for intelligent sandwich structures *Smart Mater. Struct.* **9** 32835
[42] Davì G and Milazzo A 2001 Multidomain boundary integral formulation for piezoelectric materials fracture mechanics *Int. J. Solids Struct.* **38** 7065–78
[43] Hermann G 1955 Forced motion of Timoshenko beams *ASME J. Appl. Mech.* **22** 53–6